Deregulated expression of c-Myc in a translocation-negative plasmacytoma on extrachromosomal elements that carry *IgH* and *myc* genes

Francis Wiener*, Theodore I. Kuschak†, Shinsuke Ohno‡, and Sabine Mai†§

*Microbiology and Tumorbiology Center, Karolinska Institute, Box 280, S-171 77 Stockholm, Sweden; †The Genomic Centre for Cancer Research and Diagnosis, Manitoba Institute of Cell Biology, Manitoba Cancer Treatment and Research Foundation and the University of Manitoba, 100 Olivia Street, Winnipeg, MB R3E 0V9, Canada; and ‡Department of Molecular Immunology, Cancer Research Institute Kanazawa University, 13-1, Takara-machi, Kanazawa 920, Japan

The induced expression of c-Myc in plasmacytomas in BALB/c mice is regularly associated with nonrandom chromosomal translocations that juxtapose the c-*myc* gene to one of the *Ig* loci on chromosome 12 (*IgH*), 6 (*IgK*), or 16 (*IgL*). The DCPC21 plasmacytoma belongs to a small group of plasmacytomas that are unusual in that they appear to be translocation-negative. In this paper, we show the absence of any c-*myc*-activating chromosomal translocation for the DCPC21 by using fluorescent *in situ* hybridization, chromosome painting, and spectral karyotyping. We find that DCPC21 harbors c-*myc* and *IgH* genes on extrachromosomal elements (EEs) from which c-*myc* is transcribed, as shown by c-*myc* mRNA tracks and extrachromosomal gene transfer experiments. The transcriptional activity of these EEs is supported further by the presence of the transcription-associated phosphorylation of histone H3 (H3P) on the EEs. Thus, our data suggest that in this plasmacytoma, c-Myc expression is achieved by an alternative mechanism. The expression of the c-Myc oncoprotein is initiated outside the chromosomal locations of the c-*myc* gene, i.e., from EEs, which can be considered functional genetic units. Our data also imply that other ''translocation-negative'' experimental and human tumors with fusion transcripts or oncogenic activation may indeed carry translocation(s), however, in an extrachromosomal form.

The activation of the c-*myc* gene is key to the development of all murine plasmacytomas (PCTs), resulting in deregulated levels of endogenous c-Myc protein expression (1–3). In the majority of pristane-induced mouse PCTs, the deregulation of c-*myc* transcription is achieved by chromosomal translocation that juxtaposes the c-*myc*/*pvt-1* locus on chromosome 15 to one of the *Ig* loci: on chromosome 12 (*IgH*), 6 (*IgK*), or 16 (*IgL*) (2, 3).

In a few PCTs, classical G banding analysis could not identify any of the PCT-associated typical or variant translocations (3). Molecular and cytogenetic analysis of the translocation-negative PCTs revealed that the overexpression of the c-*myc* gene was achieved by different means. c-Myc deregulation resulted from either promoter/enhancer insertion brought about by retroviral insertion into the 5′ flanking region of c-Myc (4), insertion of the *Ig* heavy chain enhancer (5), or complex genomic rearrangements (6, 7). Although less than 1% of the PCTs analyzed to date belong to the group of translocation-negative PCTs, they are of interest because they may reveal a new mechanism of plasmacytomagenesis. Consequently, the lack of cytogenetically identifiable translocations suggests alternate pathways by which c-Myc overexpression is achieved in this group of tumors.

To examine the mechanism(s) of c-Myc deregulation in translocation-negative PCTs, we focused our investigation on DCPC21, a PCT that had been induced by i.p. implantation of a plastic diffusion chamber into a BALB/c female mouse (6). Previous work by these authors had suggested that DCPC21 exhibited complex molecular rearrangements leading to the

IgH–*myc* gene juxtaposition by the insertion of the *myc*- and *pvt-1* loci-containing chromosome 15 segment into the *IgH* locus on chromosome 12 (7). The realization of such a complex rearrangement requires the occurrence of a paracentric inversion, a deletion/insertion, and multiple translocations both on chromosome and gene levels during the process of the *IgH*–*myc* illegitimate recombination (7).

Here we report that the results of classical and molecular cytogenetic analyses show that the DCPC21 PCT lacks any type of interchromosomal recombination that could cause the constitutive activation of the c-*myc* gene. However, chromosomal segments containing c-*myc* and *IgH* sequences are present— either alone or jointly—on extrachromosomal elements (EEs) in the DCPC21 PCT. We demonstrate that the deregulated expression of c-*myc* occurs on EEs, and this appears to be sufficient to sustain the malignant phenotype of the DCPC21 tumor.

Materials and Methods

Tumor Cells. DCPC21 was induced in a female BALB/c mouse by i.p. implantation of a Millipore diffusion chamber (8).

Trypsin-Giemsa Banding. Metaphase spreads were prepared without Colcemid treatment. Trypsin-Giemsa banding was performed as described previously (9) and adapted to mouse chromosomes. Chromosome identification followed the recommendations of the Committee on Standardized Genetic Nomenclature for Mice (10).

Molecular Cytogenetics. Chromosomes were analyzed by FISH (fluorescent *in situ* hybridization) as published previously (11, 12). Analysis of slides was performed by using a Zeiss Axiophot microscope, a Power Macintosh 8100 computer, and a charge-coupled device camera (Photometrics); the analytical software used was IPLABSPECTRUM 3.1 (Signal Analytics, Fairfax, VA).

FISH Probes and Detection of Hybridization. The following probes were used: c-*myc* (13), *IgH* (*pJ11*; ref. 14), and *pvt-1* (15). The probes were labeled by random priming with either digoxigenin-or biotin-dUTP (Roche Diagnostics). The detection of hybridization signals with digoxigenin-labeled probes was carried out by using a fluorescein-conjugated polyclonal sheep anti-digoxigenin antibody (Roche Diagnostics). For the detection of hybridization signals obtained with biotinylated probes, we used

MEDICAL SCIENCES

a monoclonal anti-biotin antibody (Roche Diagnostics) followed by a Texas Red-conjugated goat anti-mouse-IgG secondary antibody (Southern Biotechnology Associates).

FISH-EEs (FISH on Purified Extrachromosomal DNA Molecules). The total population of EEs was purified and examined by FISH as described (T.I.K., J. T. Paul, J. A. Wright, J. F. Mushinski, and S.M., http://www.biomednet.com/db/tto). EEs were hybridized with c-*myc*, *IgH*, and *pvt-1*. The specificity of these hybridizations was confirmed by the absence of hybridization signals with a negative control, *cyclin C* (ref. 11; T.I.K., *et al.*, http://www.biomednet.com/db/tto) and hybridization signals obtained with a positive control, *cot-1* DNA (not shown).

Chromosome Painting. The chromosome paints used (Cedarlane Laboratories) were a FITC-conjugated mouse chromosome 15 and a biotinylated mouse chromosome 12-specific paint. Hybridization of chromosome paints, alone or in combination with FISH probes, was carried out as described in the general FISH protocol. Chromosome 12 hybridization signals were detected with a monoclonal anti-biotin antibody (Roche Diagnostics) at 0.5 ng per slide followed by a Texas Red-conjugated goat anti-mouse-IgG secondary antibody (Southern Biotechnology Associates) at 2.5 ng per slide. The hybridization signals of the FITC-labeled chromosome 15 paint were amplified by using a rabbit anti-FITC antibody (Cedarlane Laboratories), followed by a FITC-labeled goat anti-rabbit IgG secondary antibody (Sigma). Both antibodies were used at 1:40 dilution.

Spectral Karyotyping (SKY). SKY was performed by using the ASI (Applied Spectral Imaging, Carlsbad, CA, and Migdal Ha'Emek, Israel) kit for mouse spectral karyotyping and the suppliers' hybridization protocols. Analyses were carried out by using the Spectra Cube on a Zeiss Axiophot 2 microscope and the SKYVIEW 1.2 software on a PC (PII-350).

mRNA Track Studies. mRNA tracks studies were carried out as described in ref. 16 on freshly isolated ascitic DCPC21 tumor cells. The cells were cytospun onto microscopic slides (10^5 cells per slide) and fixed in formaldehyde (1% in 1× PBS/50 mM MgCl$_2$). The slides were washed in 2× SSC and dehydrated sequentially in 70%, 90%, and 100% ethanol. A denatured mouse c-*myc* probe, pMycEx2, a 460-bp *Pst*I-fragment of *myc* exon 2 (gift from K. Huppi, National Institutes of Health, Bethesda, MD), was added in 50% formamide/2× SSC/50 mM phosphate buffer/10% dextran sulfate for overnight hybridization at 37°C in a humidified incubator. As expected, subsequent RNase treatment removed any hybridization signals, and hybridization to chromosomes or extrachromosomal material was achieved only after the slides had been treated with RNase and pepsin and denatured before the addition of FISH probes (see also ref. 17).

Fluorescent Immunohistochemistry. Immunohistochemistry was performed as described (12). A monoclonal anti-c-Myc antibody, 3C7 (18), was used at 20 ng per slide. Visualization of this antibody was achieved with a Texas Red-conjugated secondary goat anti-mouse IgG antibody (Southern Biotechnology Associates) at 2.5 ng per slide. A sheep anti-CORE histone antibody (United States Biological) was used at 5 ng per slide and visualized with a FITC-conjugated donkey anti-sheep IgG antibody (Sigma) at 2.75 ng per slide. The anti-histone H3P antibody used is a histone H3-phophoserine mAb from Z. Darzynkiewicz (19). It was used at 4.0 ng per slide and visualized with a Texas Red-conjugated goat anti-mouse IgG antibody (Southern Biotechnology Associates) at 2.5 ng per slide.

Southern Analysis. For Southern analyses, 10 μg of DNA from primary BALB/cRb6.15 spleen or DCPC21 tumor DNA was digested overnight with 40 units of either *Hin*dIII or *Sac*I restriction endonucleases (Roche Diagnostics) and electrophoretically separated on a 0.8% agarose gel, blotted onto Hybond XL membrane (Amersham Pharmacia), and baked at 80°C for 2 hr. Hybridizations and washes were carried out according to standard procedures (20). The probes used were c-*myc* (13), *pJ11* (14), *pvt-1* (15, 21), and *JQ2* (7).

Electroporations. Spleen cells of BALB/cRb6.15 mice were harvested for extrachromosomal gene transfer studies as follows. Green fluorescent protein (GFP, pEGFP-N1; CLONTECH) was used as a tracer molecule for determination of gene transfer efficiencies. Lymphocytes isolated from one spleen were divided into three groups: electroporation of GFP plus c-*myc*/*IgH*-carrying EEs (2.5 μg), electroporation of GFP (2.5 μg), and "mock" electroporation. Electroporations were carried out in OPTI-MEM solution (Canadian Life Technologies, Burlington, Ontario, Canada) by using 1-ml Gene Pulser cuvettes (Bio-Rad) a Bio-Rad electroporator, model 1652076, and a Bio-Rad Capacitance Extender, model 1652087. The settings used were: 960 μF, 240 V. Subsequent to electroporation, the cells were washed in complete medium [RPMI 1640 with 10% FCS (Canadian Life Technologies)] and 2 mM L-glutamine/5 units/ml penicillin/5 μg/ml streptomycin/50 μM 2-mercaptoethanol] and allowed to grow in complete medium in a humidified incubator at 37°C and in the presence of 5% CO$_2$. Twenty-four hours after gene transfer, cells were cytospun onto microscope slides (10^5 cells per slide), and c-Myc protein expression was determined in splenic B cells that also expressed GFP. A FITC-conjugated anti-B220 antibody (PharMingen) was used to visualize splenic B cells on Cytospin preparations. Fluorescent immunohistochemistry of the electroporated cells was carried out as described previously (12).

Results

DCPC21 Is a Translocation-Negative PCT Harboring Extrachromosomal Elements. Karyotyping of DCPC21 metaphase spreads by standard G banding revealed that chromosomes 15, 12, 6, and 16, regularly involved in mouse PCT-specific translocations, were not part of reciprocal translocation events (Fig. 1*a*). To confirm the results provided by G banding, DCPC21 metaphases were examined further by chromosome painting, FISH, and SKY (Fig. 1 *b–e*). Because the most frequent translocation (>90%) in pristane-induced mouse PCT transposes the c-*myc*-containing segment of chromosome 15 into the neighborhood of the *IgH* gene loci on chromosome 12 (3), chromosome painting was performed to ascertain whether chromosomes 12 and 15 are carriers of cryptic rearrangements. The painting with chromosome 15- and 12-specific probes revealed the presence of four copies of chromosome 15 (green) and chromosome 12 (red) in the majority of the DCPC21 plates analyzed. More importantly, neither chromosome 15- nor chromosome 12-derived genetic material was found to be translocated or inserted into any other chromosome of DCPC21 metaphases (Fig. 1 *b* and *c*).

When either chromosome 12 paint was combined with FISH by using a c-*myc* probe or chromosome 15 paint was used in combination with an *IgH* probe (*pJ11*), it was also evident that chromosomes 12 and 15 were not involved in reciprocal translocations (Fig. 1*d* and data not shown). However, EEs carrying either c-*myc* or *IgH* genes alone or c-*myc* and *IgH* genes jointly became apparent (Fig. 1*d*, arrow).

The possible involvement of the *IgK*- and *IgL*-carrying chromosomes 6 and 16 in *Ig*/*myc* translocation was analyzed by SKY (Fig. 1*e*). SKY corroborated the data obtained by standard cytogenetics, painting, and FISH, namely, that DCPC21 does not

Fig. 1. G banding, chromosome painting, FISH, and SKY prove that DCPC21 is a translocation-negative PCT. (*a*) G banded karyotype of DCPC21 lacking any PCT-associated chromosomal translocations involving chromosomes 12 (*IgH*), 6 (*IgK*), 16 (*IgL*), and 15 (c-*myc*). The duplicated band on one chromosome 15 (arrow) was mapped to band 15D2, where c-*myc* is located. Additional chromosomal aberrations (see ▲), such as the elongated chromosome 9 and the marker chromosome M1 as well as the centromerically fused Rb16;19 and the Rb19 isochromosome, probably are acquired during neoplastic progression (see text). (*b* and *c*) Chromosome painting of DCPC21 metaphases with chromosome 12 (red) (*b*) and with chromosome 15 paint (green) (*c*). No translocation between chromosomes 12 and 15 is visible. In addition, no chromosome 12- or 15-derived material is found as part of any other chromosome. (*d*) Painting of a DCPC21 metaphase with chromosome 12 (red) and FISH with c-*myc* (green). The arrow points a large EE that hybridizes with red and green, indicating the presence of chromosome 12-derived sequences and c-*myc* on the EE. (*e*) SKY analysis of a DCPC21 metaphase. The data are presented as follows. The image in the upper left corner of the composite shows a representative metaphase obtained with the Spectra Cube before the classification of the spectral colors. The upper center image shows the inverted 4′,6-diamidino-2-phenylindole (DAPI) banding of the same metaphase plate, and the image in the upper right corner displays the spectral colors as classified by SKYVIEW 1.2 (Applied Spectral Imaging). The lower image shows identical chromosome pairs of nonclassified and classified DCPC21 chromosomes. SKY corroborates the results of the G banding and chromosome painting: DCPC21 PCT cells do not exhibit any chromosomal translocation. SKY revealed the translocation of chromosome 16-derived material onto the telomeric part of chromosome 9 (see arrows) and the insertion of a chromosome 3-derived band into chromosome 2 (arrow). A centromeric fusion occurred between chromosomes 16 and 19 (Rb 16;19). The M1 marker contains both chromosome X- and 5-derived chromosomal segments (arrow).
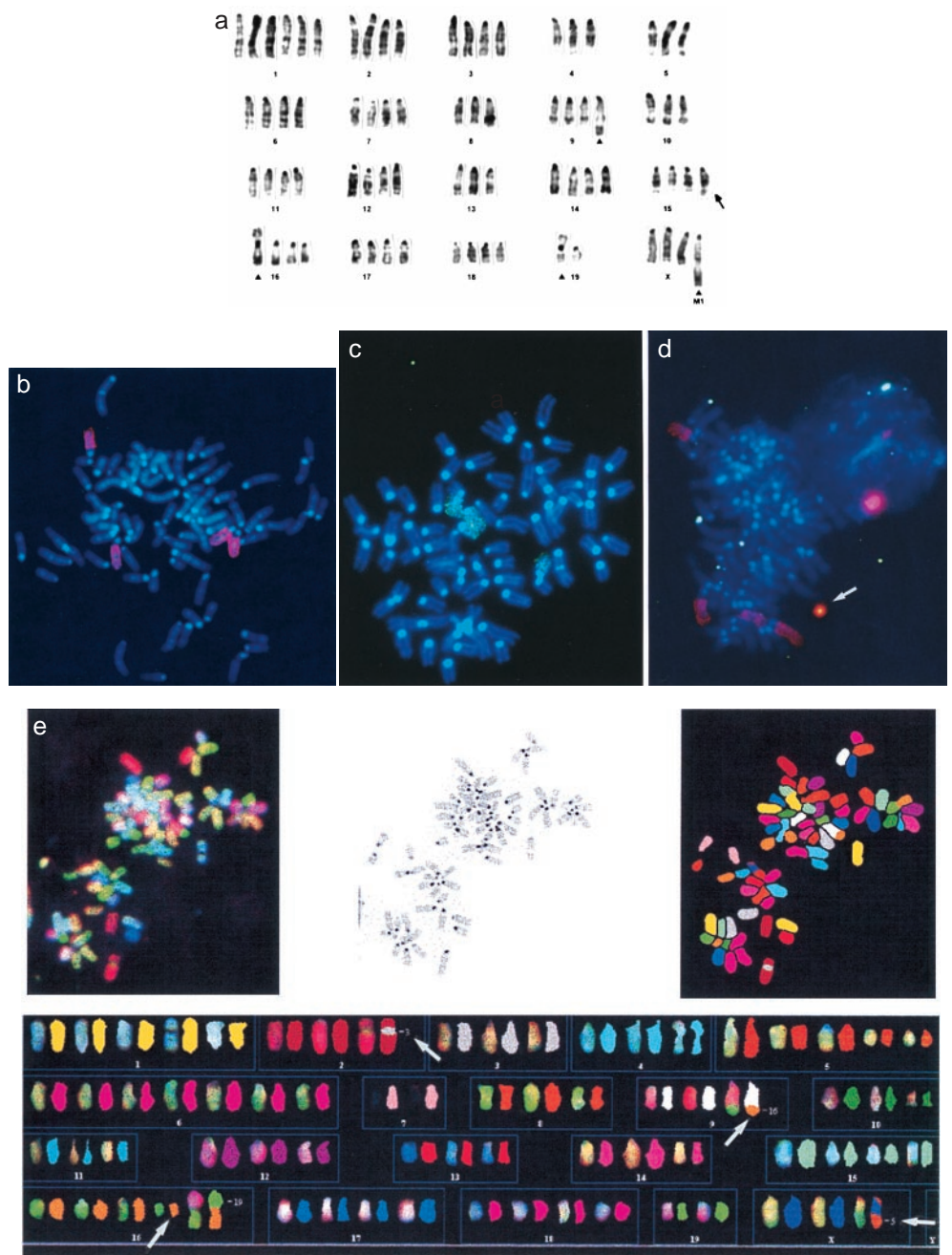

carry any PCT-associated c-*myc*-activating chromosomal translocation.

In addition, SKY revealed the nature and structure of the chromosomal aberrations detected by G banding. Noteworthy, SKY showed that the duplicated D2 band on one of the chromosomes 15 (Fig. 1*a*, arrow) contained only chromosome 15-derived genetic material (Fig. 1*e*), excluding the likelihood of an interchromosomal rearrangement involving chromosome 15. The additional band on chromosome 9 was identified as derived from chromosome 16, whereas one copy of chromosome 16 was centromerically fused with one chromosome 19. A "hidden" chromosomal aberration, undetected by classical G banding, was the insertion of chromosome 3-derived material into one chromosome 2. Because the aberrations involving chromosomes 9

and 2, as well as the fusion of chromosomes 16 and 19, were not consistently seen in all metaphases, they are likely chromosomal aberrations acquired during tumor progression, rather than during tumor initiation.

Classical cytogenetics, chromosome painting, FISH, and SKY establish that the DCPC21 PCT lacks any chromosomal aberration that reasonably could be involved in the constitutive activation of the c-*myc* gene. However, the presence of *IgH* and c-*myc* sequences on EEs suggests that these genetic entities may be responsible for the deregulation of c-Myc in this tumor.

Southern Blot Analysis Shows Rearrangements Within the *IgH* Locus and in the 5′ Flanking Region of *c-myc*. Southern blot analysis was performed with normal mouse spleen DNA and DCPC21 tumor
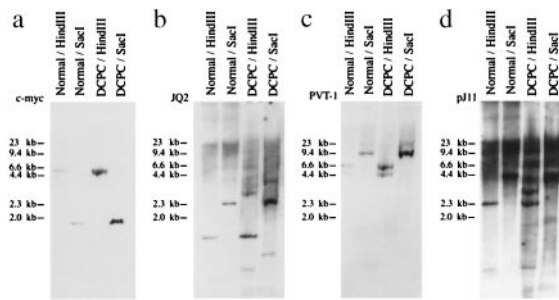
Fig. 2. Southern analysis of 10 μg of genomic DNA of DCPC21 PCT cells (''DCPC'') and normal spleen cells (''normal''). The same blot was hybridized with c-*myc* (*a*), the 5′ flanking region of c-*myc* (JQ2) (*b*), *pvt-1* (*c*), and *IgH* (pJ11) (*d*). Note that c-*myc* and *pvt-1* show germ-line hybridization signals (lanes 1–4, respectively), whereas JQ2 and pJ11 (lanes 3 and 4, respectively) indicate rearrangements (for details, see text). The stronger hybridization intensity of the c-*myc* and *pvt-1* signals (lanes 3 and 4, *a* and *c*, respectively) is consistent with the duplicated D2 band in chromosome 15 and the additional c-*myc* copies of the other 15 chromosomes (Fig. 1*a*).

DNA. The c-*myc* gene, visualized by using a mouse exon 2-specific probe, showed no rearrangement(s) and exhibited identical hybridization patterns in *Hin*dIII and *Sac*I digests of normal spleen and DCPC21 DNA (Fig. 2*a*). Similarly, *pvt-1* showed no evidence of rearrangements (Fig. 2*c*). The stronger hybridization signals of c-*myc* and *pvt-1* in DCPC21 DNA reflect both the duplication of the *myc/pvt-1*-containing 15D2 band of one chromosome 15 (Fig. 1*a*, arrow) and the additional copies of chromosome 15 (Fig. 1). In contrast to the germ-line bands observed with c-*myc* and *pvt-1*, rearrangements within the *IgH* sequences and in the 5′ flanking region of c-*myc* became apparent when using the *IgH* probe (*pJ11*) as well as a 5′ flanking probe of the c-*myc* gene (*JQ2*) (Fig. 2 *b* and *d*, respectively).

Because none of the bands that hybridized with *JQ2* cohybridized with *JQ2*, it can be excluded that any of the additional bands represent a cryptic transposition of sequences detected by *pJ11* and *JQ2*. Furthermore, a transposition of *pvt-1* and c-*myc* within the chromosomal DNA of DCPC21 is unlikely, because, as shown in Fig. 2, these two genes were not involved in translocation and or rearrangement events detectable in genomic DNA. These results suggest that the rearranged genomic bands represent intrachromosomal rearrangements, possibly because of the excision of c-*myc* and *IgH* sequences from the relevant chromosomes rather than interchromosomal recombination.

c-*myc* and *IgH* Colocalize on EEs and Are Functional Genetic Units. We consistently observed extrachromosomal c-*myc* and *IgH* hybridization signals in DCPC21 metaphases (Fig. 1). To analyze these EEs further, we performed FISH on the total population of EEs. Fig. 3 illustrates the findings for FISH-EEs hybridized with c-*myc* and *IgH* probes. In the majority of the cases, c-*myc* and *IgH* were found together on the large EEs [0.1–0.2 μm in diameter, as determined by electron microscopy (EM) measurements] (Fig. 3*d*). Notably, c-*myc* and *IgH* also were found alone on EEs of smaller sizes (0.01 μm in diameter) (Fig. 3 *b*–*d*). *pvt-1* could be detected on some of the EEs, together with c-*myc* and *IgH* (not shown).

The colocalization of c-*myc*/*IgH* on some of the EEs raised the question of whether these EEs are biologically active structures. To investigate this hypothesis, we analyzed whether these EEs were associated with active chromatin, could transcribe c-*myc* mRNA, and confer c-Myc overexpression to resting primary B cells in extrachromosomal gene transfer studies.

To determine whether the EEs contained active genes, we (*i*) first examined the presence of histones and of the transcription-
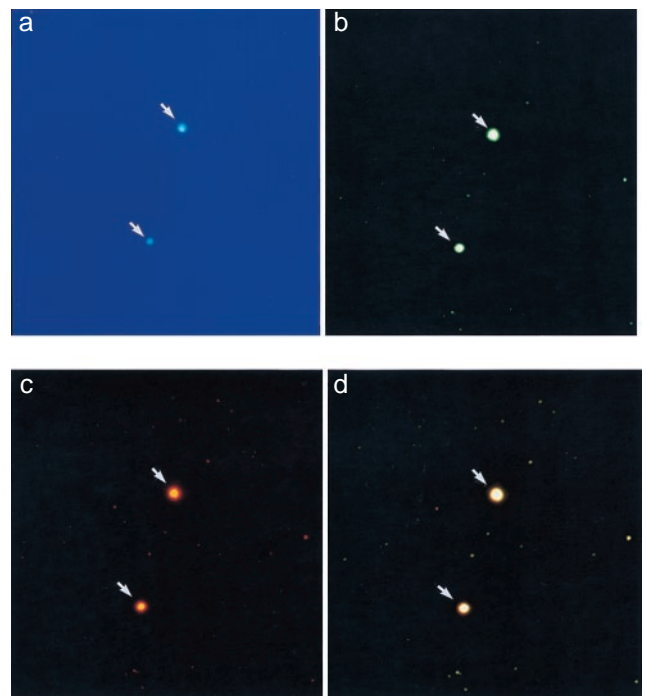

Fig. 3. FISH-EEs. Purified EEs were hybridized with c-*myc* (green) and *IgH* (pJ11, red). (*a*) DAPI counterstain of EEs. Only the large EEs are clearly visible (see arrows). (*b* and *c*) The same large EEs shown in *a* hybridized with c-*myc* (green) and *IgH* (red). (*d*) Overlay of images *b* and *c* shows the large EEs in orange (see arrows). This indicates the colocalization of the c-*myc* and *IgH* signals on the large EEs. Small EEs carry one or the other hybridization signal and, only occasionally, both. Preliminary analysis of these EEs by electron microscopy indicates that the large EEs are 0.1–0.2 μm in diameter, whereas the little ones are 0.01 μm in diameter (data not shown).

associated H3P (19, 22) on the EEs and (*ii*) then carried out mRNA track studies (Fig. 4 *a* and *b*). Using a pan-histone antibody that detects all histones irrespective of chromatin activation, we found histones on the large but not on the small EEs. To determine whether the former also were transcriptionally active, we examined the presence of H3P by using a monoclonal anti-histone H3P antibody (see *Materials and Methods*). We found that more than 90% of the pan-histone-containing EEs also stained with the monoclonal anti-histone H3P antibody, indicating that these EEs contained active chromatin (Fig. 4*a*).

To examine whether c-*myc* mRNA was produced from these EEs, we carried out mRNA track studies. As shown in Fig. 4*b*, we observed that multiple, short c-*myc* RNA tracks, typical of episomal (extrachromosomal) gene transcription (16), were generated from DCPC21-EEs. To unequivocally demonstrate that the mRNA was derived from the EEs, we processed the identical slides for FISH after RNase and pepsin treatment and after slide denaturation. Colocalizing c-*myc* mRNA (red signals) and c-*myc*-EEs DNA signals (green) are shown by arrows in Fig. 4*c*. We consistently observed that all c-*myc* mRNA tracks colocalized with EEs that showed c-*myc* DNA by FISH. However, the number of c-*myc*-carrying EEs in a DCPC21 cell was higher than the amount of EEs that were transcribing c-*myc* mRNA.

To further examine the functional activity of DCPC21 EEs, we electroporated purified EEs into normal BALB/cRb6.15 spleen cells together with a vector expressing GFP. The latter served as tracer molecule for gene transfer efficiency. The B lineage-specific marker B220 was used to determine the lineage origin of the electroporated cells. When purified DCPC21 EEs were introduced into normal BALB/cRb6.15 spleen cells, they con-
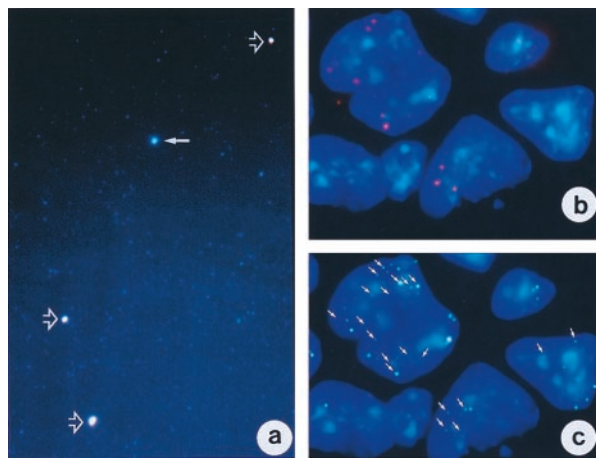
Fig. 4. The EEs are functional genetic units. (*a*) Purified extrachromosomal DNA molecules were immunostained with anti-histone antibodies. EEs are counterstained with DAPI and, therefore, appear blue. Immunostaining with the pan-histone antibody appears green, whereas the anti-histone-H3P-stained targets appear red. Thus, EEs immunostained with pan-histone antibody plus DAPI appear greenish-whitish, whereas those stained with histone H3P plus DAPI appear reddish. When histone H3P and pan-histone colocalize on the same EE, the color overlay is yellowish. The image shows four large EEs (arrows) that are surrounded by a group of small EEs. The small EEs stain with DAPI only. A pan-histone-immunostained EE is shown by a solid arrow. Three EEs indicated with open arrows show colocalization of anti-pan-histone (green) and anti-histone H3P (red) antibodies. (*b*) mRNA track study of c-*myc* in DCPC21 PCT cells. Red signals represent mRNA tracks produced in the cells. The tracks are short, as expected, from extrachromosomal DNA or episomes. (*c*) FISH analysis of the sample shown in *b*. The c-*myc* gene was labeled with digoxigenin and visualized with an anti-digoxigenin-FITC antibody (*Materials and Methods*). Arrows point to those c-*myc*-carrying EEs (green) that also transcribe c-*myc* (compare *b* and *c*). Note that not all c-*myc*-bearing EEs are transcribing c-*myc*.

ferred c-*myc* expression to GFP-expressing B220-positive B cells (Fig. 5*A*). However, within 24 hr, the DCPC-21 EEs induced cell death in the majority of the GFP-expressing B cells (>90%), whereas cells electroporated with GFP only survived. Cell death

was associated with c-Myc overexpression and visible by the appearance of apoptotic bodies (Fig. 5*B*).

Discussion

c-*myc*/*IgH*-Carrying EEs Represent an Alternative Mechanism of c-Myc Overexpression in DCPC21 PCT.
In the present study, we have shown that DCPC21 PCT lacks any of the usual chromosomal translocations associated with c-*myc* gene deregulation in PCTs. Instead, we see the presence of c-*myc* and *IgH* together on EEs in this tumor. This raised the question of whether c-Myc deregulation in this PCT was linked to the presence of these EEs. Several experiments have confirmed that the c-*myc*/*IgH*-carrying EEs express c-Myc. We have directly shown c-*myc* mRNA tracks and active chromatin-associated histone H3 phosphorylation on these EEs. This was confirmed further by gene transfer experiments of the EEs. Transfer of EEs from DCPC21 cells into primary mouse B cells resulted in increased c-Myc expression followed by apoptotic cell death. We therefore conclude that the deregulated c-Myc expression in this PCT occurred by a mechanism not involving chromosomal translocation or viral insertion. This novel pathway of c-*myc* activation involves the formation of EEs that result in c-Myc expression levels similar to that seen in *Ig*/*myc* chromosomal translocation-positive PCTs.

Extrachromosomal DNA elements have been found in all organisms analyzed to date (for review see, ref. 23). EEs may be generated transiently during normal lymphocyte development (24, 25), but the size and numbers can vary depending on genotoxic treatments (26–28). Tumor cells often harbor EEs (29, 30), and these EEs can contain oncogenes and drug-resistance genes (31–37). In a previous study, the MOPC265 PCT cell line was shown to have a T(12;15) translocation that also contained c-*myc* and *pvt-1* genes duplicated on chromosome 15 and on extrachromosomal elements (21). However, DCPC21 represents the first reported translocation-negative PCT carrying functional c-*myc*-transcribing EEs.

Model for the Generation of DCPC21-EEs Containing Both *myc*/*pvt-1* and *IgH* Sequences.
The presence of c-*myc*/*IgH*-containing EEs raises the question about the mechanism(s) for their formation in the DCPC21 PCT. One possible model that is consistent with
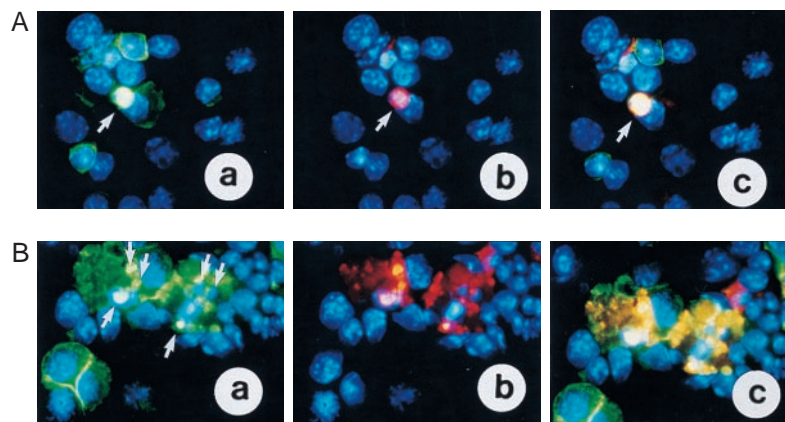
Fig. 5. Extrachromosomal gene transfer studies. Purified EEs were electroporated into primary spleen cells along with a GFP-expressing vector that served as a tracer molecule for gene transfer efficiency. B220 was used as a cell surface marker for splenic B lymphocytes. (*A*) GFP and c-Myc expression in primary B cells 24 hr after electroporation: (*a*) B220-positive primary B cells as revealed by the FITC-conjugated (green) antibody on the membrane. The arrow points to a B cell expressing GFP. The greenish-whitish color is due to the overlay of the nuclear staining with DAPI (blue) and GFP (green). (*b*) The B220-positive B cell that shows GFP expression also overexpresses c-Myc protein (red) (see arrow). (*c*) Overlay of image *a* and *b*: the orange nucleus shown expresses GFP and c-Myc (see arrow). (*B*) Ninety percent of the electroporated primary B cells die 24 hr after transfer of EEs: (*a*) GFP expression in B220-positive B cells. (*b*) c-Myc-expression in B220-positive B cells. (*c*) Overlay of *a* and *b*: the GFP-positive and B220-positive primary B cells that overexpress electroporated c-Myc die. Arrows point to some of the apoptotic bodies that form in these cells.

MEDICAL SCIENCES

the experimental data is as follows. This model assumes independent generation of *myc/pvt-1-* and *IgH*-carrying EEs followed by recombination to generate *myc/Ig*-carrying EEs. Consistent with this model, we find EEs of various sizes, some of which carry both c-*myc* and *IgH* or either gene alone. A possible source for generation of these extrachromosomal elements could be *Ig* switch recombination, because circular elements containing *Ig* sequences have been described in normal B cell development (24). EEs that confer a growth/survival advantage, such as deregulated c-Myc expression, to the cell would be selected and maintained. Because we showed increased apoptotic cell death after gene transfer of EEs into normal B cells, other genetic events also would have to occur to prevent apoptosis during plasmacytomagenesis.

Are EEs Causally Involved in Other Translocation-Negative Tumors?
EEs are present in a variety of human tumors but their role in tumor initiation or progression is still poorly understood (38–40). The importance of amplified c-*myc* or N-*myc* genes, located on double-minute chromosomes (DMs), for maintenance of tumorigenicity has been shown. Elimination of the DMs results in reduced tumorigenicity (41–43).

Other human neoplasia that normally show specific translocations also have translocation-negative subsets. Recent analysis of a series of chronic myelogenous leukemia cells revealed an incongruity between the overexpression of the oncogenic *BCR-ABL* fusion protein and the absence of cytogenetically detectable T(9;22)(q34;q11) Philadelphia (Ph) chromosome (44–49). A recent investigation of the T(11;14) translocation and the overexpression of the *MLL-AF4* fusion gene in acute lymphoblastic leukemia revealed that 7 of 18 patients the generation of the *MLL-AF4* protein occurred without detectable T(11;14) translocations (50). Burkitt lymphomas (BLs) usually contain *Ig/myc*-juxtaposed chromosomal translocations (for review, see refs. 51–53). We recently have found in a translocation-negative BL c-Myc overexpression from EEs containing c-*myc* and *IgH* sequences, without rearrangement of the chromosomal c-*myc* gene (unpublished data).

In conclusion, our results provide evidence that the EEs represent functional genetic units that may play an essential role transformation of the translocation-negative DCPC21 PCT. Our findings also suggest that other neoplasms with fusion transcripts or oncogene activation and amplification with no visible chromosomal translocations may indeed carry specific translocation(s) in an extrachromosomal form.

1. Cory, S. (1986) *Adv. Cancer Res.* **47,** 189–234.
2. Ohno, S., Babonits, M., Wiener, F., Spira, J., Klein, G. & Potter, M. (1979) *Cell* **18,** 1001–1007.
3. Potter, M. & Wiener, F. (1992) *Carcinogenesis* **13,** 1681–1697.
4. Shaughnessy, J. D., Jr., Owens, J. D., Wiener, F., Hilbert, D. M., Huppi, K., Potter, M. & Mushinski, J. F. (1993) *Oncogene* **8,** 3111–3121.
5. Fahrlander, P. D., Sumegi, J., Yang, J., Wiener, F., Marcu, K. B. & Klein, G. (1984) *Proc. Natl. Acad. Sci. USA* **81,** 7046–7050.
6. Ohno, S., Migita, S. & Murakami, S. (1989) *Oncogene* **4,** 1513–1517.
7. Ohno, S., Migita, S. & Murakami, S. (1991) *Int. J. Cancer* **49,** 102–108.
8. Merwin, R. M. & Redmon, I. W. (1963) *J. Natl. Cancer. Inst.* **31,** 998–1007.
9. Wang, H. C. & Fedoroff, S. (1971) *Nature (London)* **235,** 52–54.
10. Committee on Standardized Genetic Nomenclature for Mice (1969) *Mouse News Letter* **17,** 481–487.
11. Mai, S., Hanley-Hyde, J. & Fluri, M. (1996) *Oncogene* **12,** 277–288.
12. Fukasawa, K., Wiener, F., Vande Woude, G. F. & Mai, S. (1997) *Oncogene* **15,** 1295–1302.
13. Mai, S. (1994) *Gene* **148,** 253–260.
14. Greenberg, R., Lang, R. B., Diamond, M. S. & Marcu, K. B. (1982) *Nucleic Acids Res.* **10,** 7751–7761.
15. Huppi, K., Siwarski, D., Skurla, R., Klinman, D. & Mushinski, J. F. (1990) *Proc. Natl. Acad. Sci. USA* **87,** 6964–6968.
16. Szeles, A., Falk, K. I., Imreh, S. & Klein, G. (1999) *J. Virol.* **73,** 5064–5069.
17. Lawrence, J. B., Singer, R. H. & Marselle, L. M. (1989) *Cell* **57,** 493–502.
18. Evan, G. I., Lewis, G. K., Ramsay, G. & Bishop, J. M. (1985) *Mol. Cell. Biol.* **5,** 3610–3616.
19. Juan, G., Traganos, F., James, W. M., Ray. J. M., Roberge, M., Sauve, D. M., Anderson, H. & Darzynkiewicz, Z. (1998) *Cytometry* **32,** 71–77.
20. Sambrook, J., Fritsch, E. F. & Maniatis, T. (1989) *Molecular Cloning: A Laboratory Manual* (Cold Spring Harbor Lab. Press, Plainview, NY).
21. Mai, S., Hanley-Hyde, J., Coleman, A., Siwarski, D. & Huppi, K. (1995) *Genome* **38,** 780–785.
22. Juan, G., Traganos, F. & Darzynkiewicz, Z. (1999) *Exp. Cell Res.* **246,** 212–220.
23. Gaubatz, J. W. (1990) *Mutat. Res.* **237,** 271–292.
24. Iwasato, T., Shimizu, A., Honjo, T. & Yamagishi, H. (1990) *Cell* **62,** 143–149.
25. Matsuoka, M., Yoshida, K., Maeda, T., Usuda, S. & Sakano, H. (1990) *Cell* **62,** 35–142.
26. Cohen, S. & Lavi, S. (1996) *Mol. Cell. Biol.* **16,** 2002–2014.
27. Cohen, S., Regev, A. & Lavi, S. (1997) *Oncogene* **14,** 977–985.
28. Regev, A., Cohen, S., Cohen, E., Bar-Am, I. & Lavi, S. (1998) *Oncogene* **17,** 3455–3461.
29. Wahl, G. M. (1989) *Cancer Res.* **49,** 1333–1340.
30. Cox, D., Yuncken, C. & Spriggs, A. I. (1965) *Lancet* **2,** 55–58.
31. Fegan, C. D., White, D. & Sweeney, M. (1995) *Br. J. Haematol.* **90,** 486–488.
32. Wullich, B., Muller, H. W., Fischer, U., Zhang, K. D. & Meese, E. (1993) *Eur. J. Cancer* **29A,** 1991–1995.
33. Chen, T. L. & Manuelidis, L. (1989) *Genomics* **4,** 430–433.
34. Delinassios, J. G. & Talieri, M. J. (1983) *Experientia* **39,** 1394–1395.
35. Rowland, P., III, Pfeilsticker, J. & Hoffee, P. A. (1985) *Arch. Biochem. Biophys.* **239,** 396–403.
36. Wettergren, Y., Kullberg, A. & Levan, G. (1995) *Hereditas* **122,** 125–134.
37. Stahl, F., Wettergren, Y. & Levan, G. (1992) *Mol. Cell. Biol.* **12,** 1179–1187.
38. Trent, J., Meltzer, P., Rosenblum, M., Harsh, G., Kinzler, K., Marshal, R., Feinberg, A. & Vogelstein, B. (1986) *Proc. Natl. Acad. Sci. USA* **83,** 470–473.
39. Martinsson, T., Stahl, F., Pollwein, P., Wenzel, A., Levan, A., Schwab, M. & Levan, A. (1988) *Oncogene* **4,** 437–441.
40. Von Hoff, D. D., Needham-Van Devanter, D. R., Yucel, Y., Windle, B. E. & Wahl, G. M. (1988) *Proc. Natl. Acad. Sci. USA* **85,** 4804–4908.
41. Von Hoff, D. D., McGill, J. R., Forseth, B. J., Davidson, K. K., Bradley, T. P., Van Devanter, D. R. & Wahl, G. M. (1992) *Proc. Natl. Acad. Sci. USA* **89,** 8165–8169.
42. Eckhardt, S. G., Dai, A., Davidson, K. K., Forseth, B. J., Wahl, G. M. & Von Hoff, D. D. (1994) *Proc. Natl. Acad. Sci. USA* **91,** 6674–6678.
43. Shimizu, N., Nakamura, H., Kadota, T., Oda, T, Hirano, T. & Utiyama, H. (1994) *Cancer Res.* **54,** 3561–3567.
44. van der Plas, D. C., Hermans, A. B., Soekarman, D., Smit, E. M., de Klein, A., Smadja, N., Alimena, G., Goudsmit, R., Grosveld, R. & Hagemeijer, A. (1989) *Blood* **73,** 1038–1044.
45. Kurzrock, R., Kantarjian, H. M., Shtalrid, M., Gutterman, J. U. & Talpaz, M. (1990) *Blood* **75,** 445–452.
46. Costello, R., Lafage, M., Toiron, Y., Brunel, V., Sainty, D., Arnoulet, C., Mozziconacci, M. J., Bouabdallah, R., Gastau, J. A. & Maranichi, D. (1995) *Br. J. Hematol.* **90,** 346–352.
47. Selleri, L., Milia, G., Luppo, M., Temperani, P., Zucchini, P., Tagliafico, E., Astusi, T., Sari, M., Donelli, A. & Castoldi, G. L. (1990) *Hematol. Pathol.* **4,** 67–77.
48. Janssen, J. W., Fonatsch, C., Ludwig, W. D., Bieder, H., Maurer, J. & Bartram, C. R. (1992) *Leukemia* **6,** 463–464.
49. Estop, A. M., Sherer, C., Cieply, K., Groft, D., Burcoglu, A., Jhanwar, S. & Thomas, J. (1997) *Cancer Genet. Cytogenet.* **96,** 174–176.
50. Uckun, F. M., Herman-Hatten, K., Crotty, M. L., Sensel, M. G., Sather, H. N., Tuel-Ajlgren, L., Sarquis, M. B., Bostrom, B., Nachman, J. B., Steinherz, P. G., *et al.* (1998) *Blood* **92,** 810–821.
51. Klein, G. (1989) *Genes Chromosomes Cancer* **1,** 3–8.
52. Klein, G. (1993) *Gene* **135,** 189–196.
53. Klein, G. (1995) *Int. J. Dev. Biol.* **39,** 715–718.